Sliding Flexible Prescribed Performance Control for Input Saturated Nonlinear Systems

Yangang Yao, Yu Kang, Yunbo Zhao, Jieqing Tan, Lichuan Gu, and Guolong Shi

***Abstract*—The issue of sliding flexible prescribed performance control (SFPPC) of input saturated nonlinear systems (ISNSs) is first studied in this article. Compared to the traditional PPC (TPPC) and the finite-time PPC (FTPPC) algorithms for ISNSs, under which the performance constraint boundaries (PCBs) present the symmetrical or asymmetric "horn" shape, which leads to a large jitter in the tracking error before the system reaches steady state; and once the parameters are selected, the PCBs are fixed, when the initial state (or reference signal) changes, it is necessary to re-verify whether the initial error still satisfies the initial constraint conditions. By designing a new pair of sliding flexible PCBs (SFPCBs) associated with the initial error, a novel SFPPC algorithm is presented in this article, which presents two main advantages: 1) the SFPCBs can slide adaptively with the initial tracking error without increasing the measure of the initial PCBs, implying that the proposed SFPPC algorithm can be applied to ISNSs with arbitrary initial errors without sacrificing the initial control performance; 2) the proposed SFPPC algorithm achieves a trade-off between performance constraint and input saturation, i.e., the SFPCBs can adaptively increase when the control input exceeds the maximum allowable threshold, effectively avoiding singularity, and when the control input is within the saturation threshold range, the SFPCBs can adaptively revert back to the original PCBs. The results demonstrate that the proposed SFPPC approach can guarantee that the system output tracks the desired signal within a prescribed time, and the tracking error always kept within the SFPCBs that depend on initial error, input and output constraints. The developed algorithm is exemplified by means of simulation instances.**

***Index Terms*—Sliding flexible prescribed performance control, input saturation, performance constraint, fuzzy logic systems.**

I. INTRODUCTION

THE physical system is inevitably constrained due to factors such as physical limitations, production safety, performance requirement, and so on. The constraints can generally be classified into two categories: those pertaining to control performance, encompassing transient/steady-state performance; and those pertaining to system capacity, including state/output/input constraints. The violation of these constraints can present potential risks to system security or result in a deterioration of system performance. The control for nonlinear systems subject to different constraints has thus attracted significant research attention, and various effective control algorithms have been developed, including the barrier Lyapunov function (BLF)-based algorithms [1]–[4], the nonlinear mapping transformation (NMT)-based algorithms [5]–[10], and so on. In addition, the PPC pioneered in [11] was developed to deal with the performance constraints by designing a pair of PCBs, so as to obtain better transient/steady-state performance. The PPC algorithm was subsequently expanded to encompass nonlinear systems of various configurations [12]–[15]. The above PPC (hereinafter referred to as "TPPC") algorithms only guarantee that the tracking error satisfies the predefined tracking accuracy within an infinite time, thereby imposing certain limitations on the method's application scope. The practical expectation is that users anticipate the tracking error to converge to a predetermined level of accuracy within a finite time.

In the field of system control, it is widely considered that it is very meaningful to achieve system convergence within a finite time. Afterwards, the finite-time control (FTC) algorithms (including finite/fixed/prescribed-time control algorithms) were presented for nonlinear systems [16]–[26]. It should be noted that the FTC algorithms mentioned above can only guarantee convergence of tracking error to a neighborhood centered around zero within a finite time, and the range of this convergence domain is dependent on multiple design parameters, resulting in tracking accuracy that cannot be set in advance. Towards this end, some novel control algorithms [27]–[30] that integrate PPC and FTC were proposed, which seem like a good idea. However, this integration obviously adds some complexity to the control design. Subsequently, by designing a pair of piecewise continuous PCBs, called finite-time PCBs (FTPCBs), Liu *et al.* [31] presented a FTPPC algorithm, which can guarantee that the system output tracks the reference signal within a prescribed time with a prescribed accuracy. Then, the FTPPC algorithms were extend to nonlinear systems with different structures [32]–[36]. However, it is worth noting that TPPC and FTPPC algorithms share two inherent limitations: 1) the PCBs of the existing TPPC and FTPPC algorithms present the symmetrical or asymmetric "horn" shape (see subgraphs (a) and (b) of Fig.1), which leads to a large jitter in the tracking error before the system reaches steady state; 2) once the parameters are selected, the PCBs of the existing TPPC and FTPPC algorithms are fixed, when

This work was supported in part by the National Natural Science Foundation of China (62033012, 62103394, 62173317, 61725304 and 62303018).(*Corresponding author: Yu Kang, Lichuan Gu.*)

Y. Yao,L.Gu and G.Shi are with the School of Information and Artificial Intelligence, Anhui Agricultural University, Hefei, 230036 China, and also with Anhui Province Key Laboratory of Smart Agricultural Technology and Equipment, and Anhui Provincial Engineering Research Center for Agricultural Information Perception and Intelligent Computing.(email: ygyao@ustc.edu.cn; glc@ahau.edu.cn;shiguolongwhu.edu.cn)

Y. Kang and Y. Zhao are with the Department of Automation, University of Science and Technology of China, Hefei, 230027 China, and Y. Kang is also with Hefei University of Technology, Hefei 230601, China, and the Institute of Artificial Intelligence, Hefei Comprehensive National Science Center, Hefei 230088, China (email:kangduyu@ustc.edu.cn;ybzhao@ustc.edu.cn)

J. Tan is with School of Mathematics, Hefei University of Technology, Hefei 230601, China (e-mail:jieqingtan@hfut.edu.cn).

the initial state (or reference signal) changes, it is necessary to re-verify whether the initial error still satisfies the initial constraint conditions, if not, the new larger PCBs have to be re-selected. Obviously, the above limitations not only lead to conservative control performance, but also time and effort for each verification. Recently, some novel algorithms that attempt to address the above limitations were presented. For instance, Zhao *et al.* [37] proposed a unified control algorithm that maps the initial PCBs to the infinite boundaries, which obviously will sacrifice the transient performance of the system. Shi *et al.* [38] presented a "tube-type PCB"-based enhancing PPC (EPPC) algorithm that can effectively enhance the system's transient performance, but limitation 1) still exist. Xie *et al.* [39] presented a quantitative PPC (QPPC) algorithm that can overcome limitations 1) and 2) to a certain extent. The QPPC algorithm proposed in [39], however, assumes that the control input can be infinite, which is evidently incongruous with the requirements of the practical control system.

Ensuring that the control input is within its maximum permissible range is an intrinsic requirement of the actual control system, and failure to do so may result in degraded performance or device damage [40]–[42]. So far, many control algorithms for focused ISNSs were proposed, the core idea of which is to convert saturated input into manageable normal input through a variety of transformations. For instance, two TPPC algorithms were obtained for ISNSs [43], [44], in which an auxiliary system is constructed to address the input saturation. Shen *et al.* [45] proposed a robust FTPPC algorithm for a 2-DOF helicopter subject to input saturation. The noteworthy aspect is that the aforementioned algorithms address input saturation and performance constraint as isolate concerns, assuming their concurrent implementation. While the input saturation and performance constraint always influence each other, and often present a 'contradiction', i.e., when the control input reaches the maximum allowable threshold, replacing the actual control input with a saturation threshold typically results in the tracking error approaching or exceeding the PCBs, thereby causing a singularity issue. Conversely, if the performance constraint is excessively stringent, it will lead to input saturation. Towards this end, the relationship between performance constraint and input saturation is first established by designing an auxiliary system [46], and the balance between the two is realized. The idea was recently extended to ISNSs with unmeasurable states [47], multi-agent systems [48], time-delay systems [49] and switched systems [50]. Nevertheless, in the above methods, when the initial state or reference signal changes, it is still necessary to re-verify whether the initial error meets the initial constraints conditions, which is obviously labor-intensive and time-consuming.

Inspired by the above-mentioned observations, a natural question arises, whether a new PPC algorithm can be designed to achieve a balance between performance constraint and input saturation, while ensuring that the initial PCBs adaptively slide with the initial error, so that it can be applied to ISNSs with arbitrary bounded initial error without sacrificing the initial control performance? This article takes a step forward toward addressing this tricky but valuable problem, which has yet to be resolved in previous research. The contributions can be summarized as follows

1) Different from the TPPC algorithms [11]–[15] and FTPPC algorithms [31]–[36], among them, the PCBs present the symmetrical or asymmetric "horn" shape, which leads to a large jitter in the tracking error before the system reaches steady state; and once the parameters are selected, the PCBs are fixed, when the initial state (or reference signal) changes, it is necessary to re-verify whether the initial error still satisfies the initial constraint conditions. By designing a new pair of SFPCBs associated with the initial error, a novel SFPPC algorithm is first presented in this article. One of its advantages is that the SFPCBs can slide adaptively with the initial tracking error state without increasing the measure of the initial PCBs. In other words, the proposed SFPPC algorithm can be applied to ISNSs with arbitrary initial errors without sacrificing the initial control performance.
2) Unlike the existing PPC algorithms of ISNSs [43]–[45], which address input saturation and performance constraint as isolate concerns, ignoring the coupling between the two. In this article, the correlation between output saturation and performance constraint is established by introducing an auxiliary system, so as to realizes a trade-off between them, i.e., when the control input reaches the maximum allowable threshold, the SFPCBs will adaptively increase to mitigate the impact of input saturation on the tracking performance, so as to effectively avoid singularity, when the control input is within the saturation threshold range, the SFPCBs can adaptively revert back to the original performance boundaries. It is noted that the PPC algorithms proposed in [46]–[50] also considered the relationship between the two, while the PCBs of which are fixed, resulting in a very limited range of applications. From this point of view, the proposed SFPPC algorithm not only establishes the correlation between input saturation and performance constraint, but also has significant advantages in control performance and application range.

II. Problem Formulation and Preliminaries

A. Problem Formulation

Consider the following ISNSs

$$\begin{cases} \dot{\chi}_j = f_j\left(\bar{\chi}_j\right) + \chi_{j+1}, j = 1, \ldots, n-1 \\ \dot{\chi}_n = f_n\left(\bar{\chi}_n\right) + \mathrm{sat}\left(u\right) \\ y = \chi_1 \end{cases} \tag{1}$$

where $\bar{\chi}_n = \left[\chi_1, \ldots, \chi_n\right]^{\mathrm{T}}$ stands for the system state vector, $\bar{\chi}_j = \left[\chi_1, \ldots, \chi_j\right]^{\mathrm{T}}$. y and $\mathrm{sat}\left(u\right)$ represent the system output and input, respectively, u represents the designed controller. $f_j\left(\cdot\right)$ stands for an uncertain nonlinear continuous function with $j = 1, \ldots, n$. The control input needs to be satisfied

$$\mathrm{sat}\left(u\right) = \begin{cases} u_d \mathrm{sgn}(u), & |u| > u_d \\ u, & |u| \le u_d \end{cases} \tag{2}$$

where u_d stands for the positive saturation threshold. Employing the following estimation to address the acute angles of sat (u)

$$\operatorname{sat}(u)=g(u)+h(u) \tag{3}$$

with $g(u)=u_d\tanh(u/u_d), h(u)=\operatorname{sat}(u)-g(u)$, where $|h(u)|\leq u_d(1-\tanh(1))=\bar{h}$.

This article aims to develop a SFPPC algorithm that guarantees

1) all closed-loop signals of system (1) are semi-global bounded;

2) the system output tracks the desired signal within a prescribed time, and the tracking error always kept within the SFPCBs.

The following reasonable assumption is proposed to accomplish the above control objectives

Assumption 1. [7], [8]: The desired signal y_d and its first-order derivative is bounded and continuous.

B. Fuzzy Approximation

Lemma 1 [26]: The uncertain nonlinear function $\mathcal{F}(\mathcal{Z})$ can be approximated by a FLS as follows

$$\mathcal{F}(\mathcal{Z})=\Upsilon^{\mathrm{T}}\Omega(\mathcal{Z})+\phi(\mathcal{Z}),\quad (|\phi(\mathcal{Z})|\leq\phi,\phi\in R^{+}) \tag{4}$$

where Υ, $\Omega(\mathcal{Z})$, $\phi(\mathcal{Z})$, $\mathcal{Z}$ respectively denote weight, basis function, error and input, $\Omega(\mathcal{Z})=[\Omega_1(\mathcal{Z}),\ldots,\Omega_m(\mathcal{Z})]^{\mathrm{T}}/\sum_{j=1}^{m}\Omega_j(\mathcal{Z})$, $m\in R^{+}$, $\Omega_i(\mathcal{Z})$ is chosen as

$$\Omega_j(\mathcal{Z})=\exp\left[\frac{-(\mathcal{Z}-\vartheta_j)^{\mathrm{T}}(\mathcal{Z}-\vartheta_j)}{\iota_j{}^2}\right], j=1,\ldots,m \tag{5}$$

where ϑ_j and ι_j denote the spreads and the center vector of $\Omega_j(\mathcal{Z})$.

III. Main results

A. Sliding Flexible Performance Constraint Boundary

Firstly, we review the PCBs of the most common existing PPC algorithms (like TPPC [11] and FTPPC [35]), one side of which are usually expressed in the following form (or variations of them)

$$\rho(t)=(\rho_0-\rho_\infty)e^{-l_s t}+\rho_\infty \tag{6}$$

with ρ_0,ρ_∞,l_s be the positive design constants, and

$$\rho(t)=\begin{cases}\rho_0+\left(\rho_{T_p}-\rho_0\right)\sin^{l_\rho}\left(\frac{\pi t}{2T_p}\right), & t\in[0,T_p)\\ \rho_{T_p}, & t\in[T_p,+\infty)\end{cases} \tag{7}$$

with $\rho_0,\rho_{T_p},T_p,l_p\in R^{+}$, $\rho_0>\rho_{T_p}$ be the design parameters.

By convention, the specification for the steady/transient-state tracking performance is typically formulated in the following manner

$$-\rho(t)<e_1<\rho(t) \tag{8}$$

or

$$\begin{cases}-\delta\rho(t)<e_1<\rho(t), & e_1\geq 0\\ -\rho(t)<e_1<\delta\rho(t), & e_1<0\end{cases} \tag{9}$$

where $e_1=\chi_1-y_d$ (y_d denotes the known desired signal) stands for the tracking error, $\delta\in(0,1)$ stands for the design constant.

One can know from (6)-(9) and subgraphs (a) and (b) of Fig.1 that the TPPC algorithms and the FTPPC algorithms have the following limitations:

$\mathscr{L}_{\mathbf{1}}$) when the initial state χ_1 or reference signal y_d changes, it is necessary to re-verify whether the initial error e_1 still satisfies the initial constraint conditions (8) or (9), if not, the new larger PCBs have to be re-selected;

$\mathscr{L}_{\mathbf{2}}$) the PCBs present the symmetrical or asymmetric "horn" shape (see subgraphs (a) and (b) of Fig.1), which leads to a large jitter in the tracking error before the system reaches steady state;

$\mathscr{L}_{\mathbf{3}}$) the relationship between input saturation and performance constraint is not taken into account.

It should be noted that there are some recent approaches that attempt to address some of these limitations. For limitation $\mathscr{L}_{\mathbf{1}}$, some larger initial PCBs can be obtained by setting parameters ρ_0 in advance to satisfy a larger range of initial error; or the initial PCBs can be mapped to the infinite boundaries by introducing a mapping function [37], which obviously will sacrifice the transient performance of the system; for limitation $\mathscr{L}_{\mathbf{2}}$, the "tube-type PCB"-based EPPC [38] is an effective method, but limitation $\mathscr{L}_{\mathbf{1}}$ and limitation $\mathscr{L}_{\mathbf{3}}$ still exist; the flexible PPC (FPPC) method recently proposed [47] overcomes both limitations $\mathscr{L}_{\mathbf{2}}$ and $\mathscr{L}_{\mathbf{3}}$, but limitation $\mathscr{L}_{\mathbf{1}}$ still exist. Towards this end, this article attempts to construct a novel SFPPC algorithm to overcome the above three limitations.

In this article, the following prescribed performance should be met

$$B_l(t)<e_1<B_h(t) \tag{10}$$

where $B_h(t)$ and $B_l(t)$ respectively represent the upper and lower SFPCBs, satisfying

$$[B_l(t),B_h(t)]^{\mathrm{T}}=[b_l(t),b_h(t)]^{\mathrm{T}}+\tanh(\kappa(t))\mathbf{\Lambda} \tag{11}$$

where $[b_l(t),b_h(t)]^{\mathrm{T}}$ represents the sliding PCB (SPCB), satisfying

$$[b_l(t),b_h(t)]^{\mathrm{T}}=\rho(t)\boldsymbol{A}\boldsymbol{B}+e_1(0)\mathscr{S}(t)\boldsymbol{\mathcal{I}} \tag{12}$$

with $\boldsymbol{B}=0.5\left[1-\mathscr{N}(e_1(0)),1+\mathscr{N}(e_1(0))\right]^{\mathrm{T}},\boldsymbol{\mathcal{I}}=[1,1]^{\mathrm{T}}$ $\boldsymbol{A}=\left[\begin{smallmatrix}-1 & -\delta\\ \delta & 1\end{smallmatrix}\right]$,$\delta\in(0,1]$, $\mathscr{N}(\cdot)=1$ if $\cdot\geq 0$,$\mathscr{N}(\cdot)=-1$ if $\cdot<0$, $\rho(t)$ represent the FTPCB (7), $\mathscr{S}(t)$ stands for the following shifting function

$$\mathscr{S}(t)=\begin{cases}\left[1-\sin\left(\frac{\pi t}{2T_p}\right)\right]^{l_s}, & t\in[0,T_p)\\ 0, & t\in[T_p,+\infty)\end{cases} \tag{13}$$

where $T_p\in R^{+},l_s\geq 1$ are the design parameters.

$\tanh(\kappa(t))\mathbf{\Lambda}$ stands for the flexible additional PCB (FPCB), $\mathbf{\Lambda}=[-\lambda_1,\lambda_2]^{\mathrm{T}}$ with $\lambda_1,\lambda_2\in R^{+}$, and $\kappa(t)$ represents the output of the following auxiliary system

$$\dot{\kappa}(t)=-k_1\kappa(t)+k_2(\eta_1(t)+\eta_2(t)),\kappa(0)=0 \tag{14}$$

where $\eta_1(t)=[\operatorname{sgn}(u-u_d)+1](u-u_d),\eta_2(t)=[\operatorname{sgn}(u+u_d)-1](u+u_d)$, $k_1,k_2\in R^{+}$ are the design parameters.

Introducing the following auxiliary variable

$$\xi(t) = e_1 - e_1(0)\mathscr{S}(t). \tag{15}$$

Then (10) is equivalent to

$$\mathscr{B}_l(t) < \xi(t) < \mathscr{B}_h(t) \tag{16}$$

with $[\mathscr{B}_l(t), \mathscr{B}_h(t)]^{\mathrm{T}} = \rho(t)\boldsymbol{AB} + \tanh(\kappa(t))\boldsymbol{\Lambda}$.

Remark 1: It can be seen from (13) and (15) that $\xi(0) \equiv 0$. One can easily further know from the expressions of $\mathscr{B}_l(t)$ and $\mathscr{B}_h(t)$ that no matter what value $e_1(0)$ takes, (16) is always true for $t = 0$, which means that the limitation $\mathscr{L}_1$ in existing TPPC algorithms [11]–[15] and FTPPC algorithms [31]–[36] is removed. Furthermore, it is worth noting that the proposed SFPPC approach is fundamentally different from the existing approaches [6], [37] that also remove limitation $\mathscr{L}_1$ at the expense of initial tracking performance. Among them, the PCBs in the initial time period are actually transformed into the infinite boundaries (i.e., unconstrained), which causes the tracking error to jitter significantly in the initial time period. However, in this article, it can be known from (10)-(14) that the initial PCB is $[-\delta\rho_0 + e_1(0), \rho_0 + e_1(0)]^{\mathrm{T}}$ for $e_1(0) \geq 0$, and the initial PCB is $[-\rho_0 + e_1(0), \delta\rho_0 + e_1(0)]^{\mathrm{T}}$ for $e_1(0) < 0$. Obviously, the measure of the initial PCB proposed in this article is $(1+\delta)\rho_0$, which is less than or equal to the measure of the original PCB (i.e., $2\rho_0$). In other words, the proposed SFPPC method still maintains good initial transient performance while removing limitation $\mathscr{L}_1$.

Remark 2: It should be noted that the PCBs of the existing TPPC algorithms [11]–[15] and FTPPC algorithms [31]–[36] present the symmetrical or asymmetric "horn" shape (see subgraphs (a) and (b) of Fig.1), which leads to a large jitter in the tracking error before the system reaches steady state (i.e., limitation $\mathscr{L}_2$). Formally, however, the PCBs proposed in this article "slide" adaptively with the initial error state without sacrificing the initial transient performance, so we visually call it "SFPCB". In addition, without considering input saturation (i.e, $\boldsymbol{\Lambda} = \boldsymbol{0}$), when $t \geq T_p$, the SPCB becomes $[-\delta\rho_{T_p}, \rho_{T_p}]^{\mathrm{T}}$ for $e_1(0) \geq 0$, or $[-\rho_{T_p}, \delta\rho_{T_p}]^{\mathrm{T}}$ for $e_1(0) < 0$, which means that the system output can track the desired signal within a prescribed time with a prescribed accuracy.

Remark 3: In fact, the SFPCB designed in this article is composed of SPCB and FPCB, i.e, $[b_l(t), b_h(t)]^{\mathrm{T}}$ and $\tanh(\kappa(t))\boldsymbol{\Lambda}$. The SPCB is to ensure the transient/steady-state of the system (see Remarks 1-2); the FPCB is designed to maintain controllability when saturation occurs. According to the expressions of $\eta_1(t)$, $\eta_2(t)$, one know that $\eta_1(t)+\eta_2(t) \geq 0$. Since $\kappa(0) = 0$, one can further obtain from (14) that $\kappa(t) \geq 0$ for $\forall t \geq 0$, and if and only if $|u| > u_d$, $\eta_1(t) + \eta_2(t) > 0$, while when $|u| \leq u_d$, $\eta_1(t) + \eta_2(t) \equiv 0$, implying that once $u > u_d$, the SFPCBs will adaptively increase to avoid singularity, and the SFPCBs will adaptively revert to the original SPCBs as the control input returns to the saturation threshold range. Fig. 1 shows the schematic diagram of tracking errors and their PCBs under TPPC, FTPPC, SFPPC with $\boldsymbol{\Lambda} = \boldsymbol{0}$, and SFPPC with $\boldsymbol{\Lambda} \neq \boldsymbol{0}$, respectively.

- Subgraphs (a) and (b) of Fig. 1 show the schematic diagram of tracking errors and their PCBs under TPPC approaches [11]–[15] and the FTPPC approaches [31]–[36], respectively. Obviously, the PCBs of the above approaches present the symmetrical or asymmetric "horn"shape, which leads to a large jitter in the tracking error before the system reaches steady state; in addition, once the parameters are selected, the PCBs are fixed, meaning that when the initial state (or reference signal) changes, it is necessary to re-verify whether the initial error $e_1(0)$ still satisfies the initial constraint conditions, if not, a new set of parameters need to be selected to satisfy the initial constraint, which is undoubtedly time-consuming and laborious.
- In subgraph (c) of Fig. 1, the SPCBs are the special form of the proposed SFPCBs (without considering the input saturation, i.e., $\boldsymbol{\Lambda} = \boldsymbol{0}$). Compare with the TPPC approaches and FTPPC approaches, its significant advantage is that the initial SPCBs can adaptively slide according to the initial error state, and the measure of the initial SPCBs is less than or equal to the measure of the original PCBs. In other words, the proposed method can be applied to ISNSs with arbitrary initial errors without sacrificing the initial control performance.
- Subgraph (d) of Fig. 1 gives the schematic diagram under the proposed SFPPC approach. In addition to including the excellent properties of SPCBs, the proposed SFPPC approach also takes into account the internal correlation between performance constraint and input saturation. In fact, when input saturation occurs, the tracking performance is bound to weaken. In this case, if the original PCBs are used, the tracking error will contact or even exceed the PCBs, resulting in the system losing control. The designed SFPCBs, however, have the capability to automatically adjust based on the relationship between the control input and the saturation threshold, i.e., when the control input exceeds the saturation threshold, the SFPCBs will adaptively expansion according to the difference between the control input and the saturation threshold to mitigate the impact of input saturation on the tracking performance, so as to effectively avoid singularity, when the control input is within the saturation threshold range, the SFPCBs can adaptively revert back to the original SPCBs.

B. Sliding Flexible Prescribed Performance Control Design

Design the following NMT

$$s(t) = \ln\left(\frac{\zeta(t)}{1-\zeta(t)}\right) \tag{17}$$

where $\zeta(t) = (\xi(t) - \mathscr{B}_l(t)) / (\mathscr{B}_h(t) - \mathscr{B}_l(t))$.

It can be obtained from the expression of $\zeta(t)$ that $\zeta(0) \in (0,1)$. According to (17), one can obtain that $s(t) \to \infty$ only and only if $\zeta(t) \to 1^-$ or $\zeta(t) \to 0^+$. It means that as long as $s(t)$ is bounded, then $\zeta(t) \in (0,1)$ holds for $\forall t \geq 0$. $\zeta(t) \in (0,1)$ means $\xi(t) \in (\mathscr{B}_l(t), \mathscr{B}_h(t))$. On the basis of (15) and (16), one can further obtain that as long as $s(t)$ is bounded, then (10) is always true, i.e., $B_l(t) < e_1 < B_h(t)$ for $\forall t \geq 0$. It means that the introduction of NMT (17)

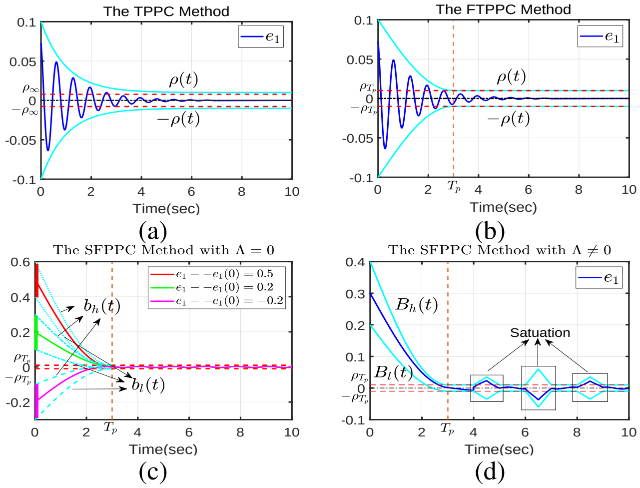

Fig. 1: Schematic diagram of four different forms of PCB.

transforms the performance constraint problem (10) into the boundedness problem for $s(t)$.

Remark 4: The NMT-based method is a common method to deal with constraint problems (including state/output and performance constraints, etc.), similar methods see [1]–[5] and their references. The core idea is to transform the constraint problem into the bounded problem of controlling auxiliary variables. Note that before using this method, it is necessary to verify whether the initial error (or state) is within the initial constraint boundaries. If not, it is necessary to increase the initial constraint range to ensure this condition, which increases the complex verification process and sacrifices the initial control performance. In fact, from a formal point of view, $\zeta(0) \in (0,1)$ must also be satisfied in this article. However, based on the above analysis, we know that $\zeta(0) \in (0,1)$ is always true in this article regardless of the value of $e_1(0)$, which further verifies that by designing the new SFPCBs related to the initial error state (11), the proposed SFPPC approach can be applied to ISNSs with arbitrary initial errors without sacrificing the initial control performance.

In the following sections, for simplicity's sake, let $B_l(t) = B_l, B_h(t) = B_h$, $\mathscr{B}_l(t) = \mathscr{B}_l, \mathscr{B}_h(t) = \mathscr{B}_h$, $\xi(t) = \xi$, $\zeta(t) = \zeta$, $s(t) = s$, $\mathscr{S}(t) = \mathscr{S}$.

Construct the error variables as follows

$$\begin{cases} z_1 = s \\ z_j = \chi_j - \alpha_{j-1}, j = 2, \ldots, n-1 \\ z_n = \chi_n - \alpha_{n-1} - o, \\ \tilde{\Psi}_j = \Psi_j - \hat{\Psi}_j, j = 1, \ldots, n \end{cases} \tag{18}$$

where α_j denotes the virtual control function, o denotes an auxiliary signal, which will be given later. $\hat{\Psi}_j$ denotes the estimation of Ψ_j, $\Psi_j = \|\Upsilon_j\|^2$.

Step 1: Select the first LF candidate (LFc) V_1 as follows

$$V_1 = \frac{1}{2} z_1^2 + \frac{1}{2r_1} \tilde{\Psi}_1^2 \tag{19}$$

where $r_1 \in R^+$ denotes a design constant.

According to (17) and (18), one can obtain

$$\dot{z}_1 = \mu \dot{e}_1 + \Gamma \tag{20}$$

where

$$\mu = \frac{1}{\zeta(1-\zeta)(\mathscr{B}_h - \mathscr{B}_l)}$$

$$\Gamma = \frac{\mu\left[\dot{\mathscr{B}}_l(\xi - \mathscr{B}_h) - \dot{\mathscr{B}}_h(\xi - \mathscr{B}_l)\right]}{\mathscr{B}_h - \mathscr{B}_l} - \mu e_1(0)\dot{\mathscr{S}}.$$

Combining (1), (18) with (20), one can obtain

$$\dot{z}_1 = \mu\left(f_1(\chi_1) + z_2 + \alpha_1 - \dot{y}_d + \frac{\Gamma}{\mu}\right). \tag{21}$$

Based on (19) and (21), one has

$$\dot{V}_1 = \mu z_1 (\mathcal{F}_1(\mathcal{Z}_1) + \alpha_1) - \mu^2 z_1^2 - \frac{\tilde{\Psi}_1 \dot{\hat{\Psi}}_1}{r_1} \tag{22}$$

where $\mathcal{Z}_1 = [\bar{\chi}_2, y_d]^{\mathrm{T}}$, $\mathcal{F}_1(\mathcal{Z}_1) = f_1(\chi_1) + z_2 - \dot{y}_d + \Gamma/\mu + \mu z_1$.

On the basis of Lemma 1, we use a FLS to approximate $\mathcal{F}_j(\mathcal{Z}_j)$, i.e., $\mathcal{F}_j(\mathcal{Z}_j) = \Upsilon_j^{\mathrm{T}} \Omega_j(\mathcal{Z}_j) + \phi_j(\mathcal{Z}_j)$, where $|\phi_j(\mathcal{Z}_j)| \le \phi_j$, and $\phi_j \in R^+$ with $j = 1, 2, \ldots, n$.

In the light of the mean inequality and $0 < \Omega_j^{\mathrm{T}}(\cdot)\Omega_j(\cdot) \le 1$, one can derive

$$\mu z_1 \mathcal{F}_1(\mathcal{Z}_1) \le \frac{\mu^2 z_1^2 \Psi_1}{2a_1 \|\Omega_1(\mathbb{Z}_1)\|^2} + \mu^2 z_1^2 + \Delta_1 \tag{23}$$

where $\Delta_1 = a_1/2 + \phi_1^2/4$, $a_1 \in R^+$,$\mathbb{Z}_1 = [\chi_1, y_d]^{\mathrm{T}}$.

Design α_1 and $\dot{\hat{\Psi}}_1$ as follows

$$\alpha_1 = -\frac{c_1 z_1}{\mu} - \frac{\mu z_1 \hat{\Psi}_1}{2a_1 \|\Omega_1(\mathbb{Z}_1)\|^2} \tag{24}$$

$$\dot{\hat{\Psi}}_1 = \frac{r_1 \mu^2 z_1^2}{2a_1 \|\Omega_1(\mathbb{Z}_1)\|^2} - \sigma_1 \hat{\Psi}_1 \tag{25}$$

where $c_1, \sigma_1 \in R^+$ denote the design constants.

Substituting (23)-(25) to (22), one can further derive

$$\dot{V}_1 \le -c_1 z_1^2 + \frac{\sigma_1}{r_1} \tilde{\Psi}_1 \hat{\Psi}_1 + \Delta_1. \tag{26}$$

Step j $(j = 2, \ldots, n-1)$: Choose the jth LFc V_j as

$$V_j = \frac{1}{2} z_j^2 + \frac{1}{2r_j} \tilde{\Psi}_j^2 + V_{j-1} \tag{27}$$

where $r_j \in R^+$denotes a design constant.

Then, one has

$$\begin{aligned} \dot{V}_j &= z_j(f_j(\bar{\chi}_j) + z_{j+1} - \dot{\alpha}_{j-1} + \alpha_j) - \frac{\tilde{\Psi}_j \dot{\hat{\Psi}}_j}{r_j} + \dot{V}_{j-1} \\ &\le z_j(\mathcal{F}_j(\mathcal{Z}_j) + \alpha_j) - z_j^2 - \frac{\tilde{\Psi}_j \dot{\hat{\Psi}}_j}{r_j} + \dot{V}_{j-1} \end{aligned} \tag{28}$$

where $\mathcal{F}_j(\mathcal{Z}_j) = f_j(\bar{\chi}_j) + z_{j+1} - \dot{\alpha}_{j-1} + z_j$, $\mathcal{Z}_j = [\bar{\chi}_{j+1}, y_d]^{\mathrm{T}}$.

Similar to (23), one can derive

$$z_j \mathcal{F}_j(\mathcal{Z}_j) \le \frac{z_j^2 \Psi_j}{2a_j \|\Omega_j(\mathbb{Z}_j)\|^2} + z_j^2 + \Delta_j \tag{29}$$

where $\Delta_j = a_j/2 + \phi_j^2/4$, $\mathbb{Z}_j = [\bar{\chi}_j, y_d]^{\mathrm{T}}$,$a_j \in R^+$.

Design α_j and $\dot{\hat{\Psi}}_j$ as follows

$$\alpha_j = -c_j z_j - \frac{z_j \hat{\Psi}_j}{2a_j \|\Omega_j(\mathbb{Z}_j)\|^2} \tag{30}$$

$$\dot{\hat{\Psi}}_j = \frac{r_j z_j^2}{2a_j \|\Omega_j(\mathbb{Z}_j)\|^2} - \sigma_j \hat{\Psi}_j \tag{31}$$

where $c_j, \sigma_j \in R^+$ denote the design parameters.

Substituting (29)-(31) into (28), we can further derive

$$\dot{V}_j \leq -\sum_{m=1}^{j} c_m z_m^2 + \sum_{m=1}^{j} \frac{\sigma_m}{r_m} \tilde{\Psi}_m \hat{\Psi}_m + \sum_{m=1}^{j} \Delta_m. \tag{32}$$

Step n: Introducing the following auxiliary system to counteract the impact of input saturation

$$\dot{o} = -o + (g(u) - u). \tag{33}$$

The nth LFc V_n is selected as

$$V_n = \frac{1}{2} z_n^2 + \frac{1}{2r_n} \tilde{\Psi}_n^2 + V_{n-1} \tag{34}$$

where $r_n \in R^+$ denotes a design constant.

Then, we have

$$\begin{aligned}\dot{V}_n =& z_n \left(f_n(\bar{\chi}_n) + h(u) + u - \dot{\alpha}_{n-1} + o\right) \\ & - \frac{\tilde{\Psi}_n \dot{\hat{\Psi}}_n}{r_n} + \dot{V}_{n-1}.\end{aligned} \tag{35}$$

In accordance with Young's inequality, we can derive

$$z_n h(u) \leq \frac{z_n^2}{4} + \bar{h}^2 \tag{36}$$

Substituting (36) to (35), one has

$$\begin{aligned}\dot{V}_n \leq& \dot{V}_{n-1} + z_n \left(u + \mathcal{F}_n(\mathcal{Z}_n) + o\right) \\ & + \bar{h}^2 - z_n^2 - \frac{\tilde{\Psi}_n \dot{\hat{\Psi}}_n}{r_n}\end{aligned} \tag{37}$$

where $\mathcal{F}_n(\mathcal{Z}_n) = f_n(\bar{\chi}_n) - \dot{\alpha}_{n-1} + (5z_n)/4$, $\mathcal{Z}_n = [\bar{\chi}_n, y_d]^{\mathrm{T}}$.

Similar to (23) and (29), one has

$$z_n \mathcal{F}_n(\mathcal{Z}_n) \leq \frac{z_n^2 \Psi_n}{2a_n \|\Omega_n(\mathbb{Z}_n)\|^2} + z_n^2 + \bar{\Delta}_n \tag{38}$$

where $\bar{\Delta}_n = a_n/2 + \phi_n^2/4$, $a_n \in R^+$,$\mathbb{Z}_n = \mathcal{Z}_n$.

Design v and $\dot{\hat{\Psi}}_n$ as follows

$$u = -c_n z_n - o - \frac{z_n \hat{\Psi}_n}{2a_n \|\Omega_n(\mathbb{Z}_n)\|^2} \tag{39}$$

$$\dot{\hat{\Psi}}_n = \frac{r_n z_n^2}{2a_n \|\Omega_n(\mathbb{Z}_n)\|^2} - \sigma_n \hat{\Psi}_n \tag{40}$$

where $c_n, \sigma_n \in R^+$.

Substituting (38)-(40) into (37), one can derive

$$\dot{V}_n \leq -\sum_{m=1}^{n} c_m z_m^2 + \sum_{m=1}^{n} \frac{\sigma_m \tilde{\Psi}_m \hat{\Psi}_m}{r_m} + \sum_{m=1}^{n} \Delta_m \tag{41}$$

with $\Delta_n = \bar{\delta}_n + \bar{h}^2$.

Bearing in mind $\tilde{\Psi}_j \hat{\Psi}_j \leq -\tilde{\Psi}_j^2/2 + \Psi_j^2/2$, one can derive

$$\dot{V}_n \leq -\sum_{m=1}^{n} c_m z_m^2 - \sum_{m=1}^{n} \frac{\sigma_m \tilde{\Psi}_m^2}{2r_m} + \Delta \tag{42}$$

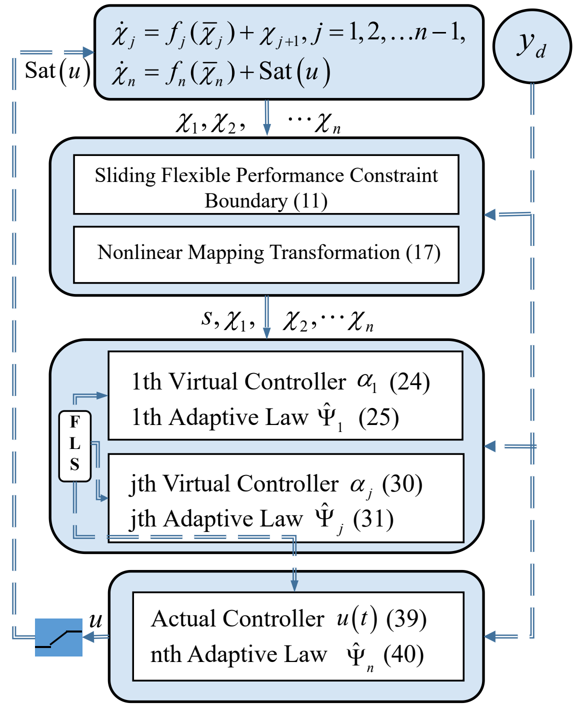

Fig. 2: The block diagram of the presented SFPPC algorithm.

where $\Delta = \sum_{m=1}^{n} \Delta_m + \sum_{m=1}^{n} \left(\sigma_m \Psi_m^2\right) / (2r_m)$.

Define $c = \min_{1 \leq m \leq n} \{2c_m, \sigma_m\}$, then one can obtain

$$\dot{V}_n \leq -cV_n + \Delta. \tag{43}$$

Fig.2 gives the block diagram of the proposed SFPPC algorithm.

C. Stability Analysis

Theorem: Consider ISNSs (1) with Assumption 1, for any bounded initial error $e_1(0)$, the SFPPC algorithm proposed in this article can guarantee that

1) All closed-loop signals in system (1) are semi-globally bounded.
2) the system output can track the desired signal within a prescribed time, and the tracking error always kept within the SFPCBs that depend on initial error, input and output constraints.

Proof: 1) According to (43), we can derive

$$\begin{aligned}V_n \leq& V_n(0) e^{-ct} + \frac{\Delta}{c} \\ \leq& V_n(0) + \frac{\Delta}{c}.\end{aligned} \tag{44}$$

From the definition of V_n and (44), one can know that z_j and $\tilde{\Psi}_j$ are bounded. On account of (2),(18),(24)-(25),(30)-(31) and (39)-(40), one can obtain that α_j ,u and $\hat{\Psi}_j$ are bounded. Since $z_1 = s, z_j = \chi_j - \alpha_{j-1}$, so s and χ_j are bounded. Accordingly, all the closed-loop signals in system (1) are semi-globally bounded.

2) In accordance with the definition of V_n and (44), one can further derive

$$|z_1| = |s| \leq \sqrt{2\left(V_n(0) + \frac{\Delta}{c}\right)} \tag{45}$$

which means that s is bound. One can obtain from the expression of $\zeta(t)$ that $\zeta(0) \in (0, 1)$. Combining the boundedness of s and (17), one can further obtained that

$$0 < \zeta(t) < 1, \forall t \geq 0. \tag{46}$$

According to the expression of $\zeta(t)$ and (46), one know that

$$\mathscr{B}_l(t) < \xi(t) < \mathscr{B}_h(t), \forall t \geq 0. \tag{47}$$

On the basis of the expression of $\xi(t)$ and (47), one can further know that

$$B_l(t) < e_1(t) < B_h(t), \forall t \geq 0. \tag{48}$$

According to the expression of $B_l(t)$ and $B_h(t)$, one can know that the system output can track the desired signal with a given accuracy within a prescribed time. Meanwhile, the tracking error always kept within the SFPCBs that depend on initial error, input and output constraints. ■

IV. Simulation

Example 1 (Theoretical system): Give a ISNS as follows

$$\begin{cases} \dot{\chi}_1 = f_1(\chi_1) + \chi_2 \\ \dot{\chi}_2 = f_2(\bar{\chi}_2) + \text{sat}(u) \\ y = \chi_1 \end{cases} \tag{49}$$

where $f_1(\chi_1) = \sin\chi_1^2 \cos\chi_1$, $f_2(\bar{\chi}_2) = -1.2\chi_1\chi_2 + \chi_1(1 + \chi_2^2)\sin\chi_2$. Select the design parameters as $c_1 = 10, c_2 = 5, a_j = 1, r_j = 10, \sigma_j = 1$ with $j = 1, 2$, $u_d = 1.5$, $\rho_0 = 0.1$, $\rho_{T_p} = 0.01$, $T_p = 5$, $l_p = l_s = 1$, $\delta = 1$, $\lambda_1 = \lambda_2 = 0.1$, $k_1 = 5, k_2 = 0.5$. Let $y_d = 0.2\sin(0.5t)$, and $\hat{\bar{\Psi}}_2(0) = [3, 2]^{\mathrm{T}}$.

In order to verify the validity of the proposed SFPPC approach, we select three different initial errors, case 1: $e_1(0) = -0.2$; case 2: $e_1(0) = 0.2$; case 3: $e_1(0) = 0.4$. Fig.3 gives the tracking curves under three different initial errors, implying that for any bounded initial errors, the proposed SFPPC algorithm ensures that the system output tracks the desired signal with a given accuracy within a prescribed time. Subgraphs (a1),(b1) and (c1) in Fig.4 show the tracking error curves and corresponding SFPCBs under three different initial errors respectively, and Subgraphs (a2),(b2) and (c2) in Fig.4 respectively show the corresponding control input curves under three conditions, implying that the tracking error always kept within the SFPCB that depend on initial error, input and output constraints. In particular, from subgraphs (a1),(b1) and (c1), we can see that when the initial error changes, the measure of the initial SFPCBs does not increase, and when the control input exceeds the saturation threshold, the SFPCBs will adaptively increase to avoid singularity, when the control input is within the saturation threshold range, the SFPCBs can adaptively revert back to the original performance boundaries.

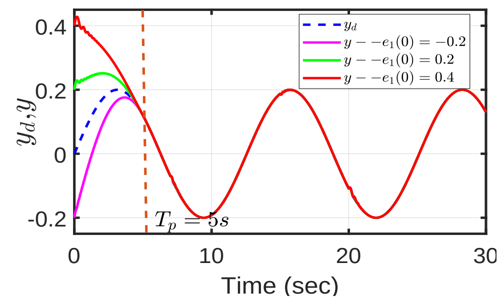

Fig. 3: Tracking curves under three different initial errors.

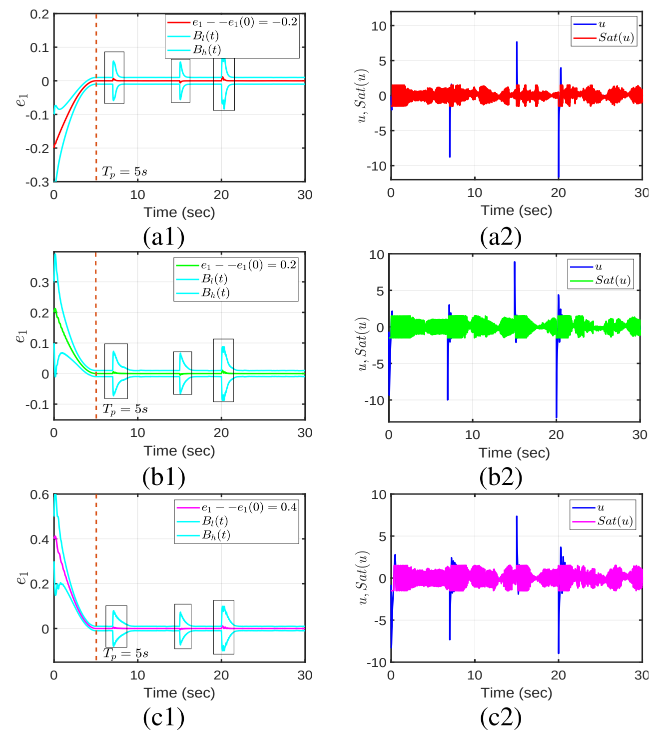

Fig. 4: (aj)(bj)(cj) with $j = 1, 2$ represent tracking error curves and control input curves under the three initial error conditions $e_1(0) = -0.2, e_1(0) = 0.2$, and $e_1(0) = 0.4$, respectively.

The proposed SFPPC method is compared with three existing PPC methods (i.e., TPPC [11], FTPPC [35] and EPPC [38]) to validate its superiority, and assume that the control input can be infinitely large for the sake of fairness. The simulation results are shown in Fig. 5. Subgraphs (a),(b) and (c) in Fig. 5 show the curves of the tracking errors and their PCBs under TPPC, FTPPC and EPPC respectively. It can be seen from subgraphs (a) and (b) in Fig. 5 that the PCBs of TPPC and FTPPC present a symmetrical or asymmetric "horn" shape, which may lead to a large jitter in the tracking error before the system reaches steady state, while one can seen from subgraph (c) in Fig. 5 that the EPPC method proposed in [38] can effectively improve this deficiency. However, it is worth noting that all three methods have an inherent limitation, i.e., once the parameters are selected, the PCBs are fixed, which further requires that the initial error must be within the initial PCBs. It means that when the initial state or reference signal changes, it is necessary to re-verify whether the initial error still satisfies the initial constraint conditions, if not, the

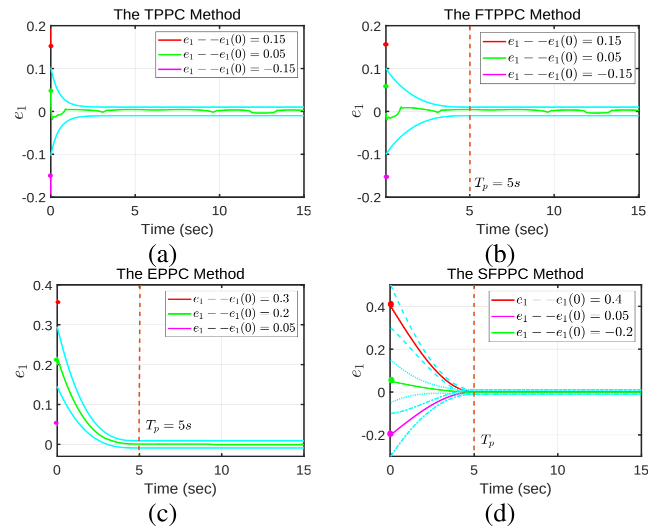

Fig. 5: (a)-(d) represent the tracking error curves and their PCBs under TPPC, FTPPC, EPPC and SFPPC with different initial conditions respectively.

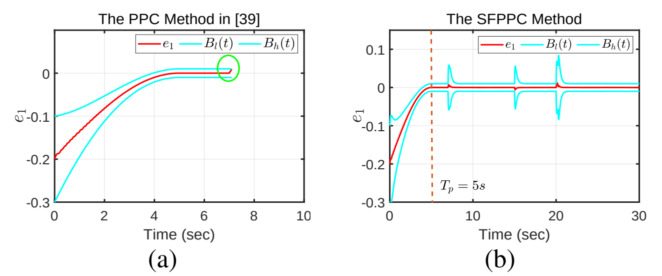

Fig. 6: (a)(b) respectively represent the tracking error curves of the PPC method in [39] and the proposed SFPPC method.

methods will fail, then the new larger PCBs has to be re-selected. One can see from subgraph (d) in Fig. 5 that the presented SFPCBs have the advantage of adaptive "sliding" the initial PCBs according to the initial error, which means that the initial PCBs will adaptively envelope the tracking error with the change of the initial tracking error, indicating that the presented SFPPC approach is appropriate for ISNSs with any bounded initial error. In particular, the measure of the initial SFPCBs proposed in this article is less than ($\delta \in (0, 1)$) or equal ($\delta = 1$) to the measure of the original PCBs, implying that the presented SFPPC approach still maintains good initial transient performance while removing the limitation existing in TPPC [11], FTPPC [35] and EPPC [38] methods.

The proposed SFPPC method is further validated for its "flexibility" by comparing it with the method in [39], which also has the ability to slide the initial PCBs. In fact, a significant advantage of the proposed SFPPC method compared with the method proposed in [39] is that it takes into account the inevitable input saturation problem in real systems, and the proposed SFPPC method reasonably establishes an organic relationship between input saturation and performance constraint. From Fig.6, one can see that when the input is saturated, the singularity will appear under the PPC method proposed in [39], resulting in the termination of simulation, while the proposed SFPPC method is still valid.

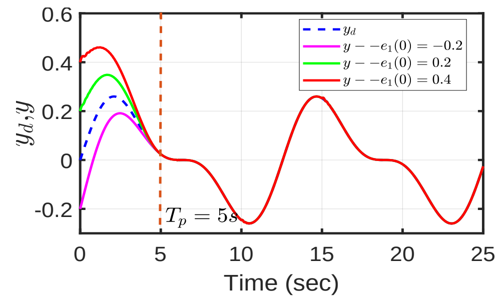

Fig. 7: Tracking curves under three different initial errors.

Example 2 (Practical system): Consider a single-link robot arm system [7] modeled with the following dynamic equation

$$\begin{cases} \dot{\chi}_1 = \chi_2 \\ \dot{\chi}_2 = \frac{\text{sat}(u)}{M} - \frac{mgl\sin\chi_1}{2M} - \frac{B\chi_2}{M} \\ y = \chi_1 \end{cases} \tag{50}$$

where $m = 0.02kg, g = 9.8m/s^2, l = 1m, M = 1kg, B = 1$. Select the design parameters as $c_1 = 10, c_2 = 5, a_j = 1, r_j = 10, \sigma_j = 1$ with $j = 1, 2$, $u_d = 1.5$, $\rho_0 = 0.1$, $\rho_{T_p} = 0.01$, $T_p = 5$, $l_p = l_s = 1$, $\delta = 1$, $\lambda_1 = \lambda_2 = 0.1$, $k_1 = 5, k_2 = 0.5$. Let $y_d = 0.2\,(0.5\sin(t) + \sin(0.5t))$, and $\hat{\Psi}_2(0) = [3, 2]^{\mathrm{T}}$. We also select three different initial errors, case 1: $e_1(0) = -0.2$; case 2: $e_1(0) = 0.2$; case 3: $e_1(0) = 0.4$. Fig.7 gives the tracking curves under three different initial errors, and subgraphs (aj)(bj)(cj) in Fig.8 with $j = 1, 2$ represent tracking error curves and control input curves under the three initial error conditions $e_1(0) = -0.2, e_1(0) = 0.2$, and $e_1(0) = 0.4$, respectively, implying that for any bounded initial errors, the proposed SFPPC algorithm ensures that y tracks y_d with a given accuracy within T_p, and e_1 always kept within the SFPCBs that depend on initial error, input and output constraints.

Similarly, we also compare the proposed SFPPC method with three existing PPC methods (i.e., TPPC [11], FTPPC [35] and EPPC [38]), and assume that the control input can be infinitely large for the sake of fairness. Subgraphs (a)-(d) in Fig. 9 show the curves of the tracking errors and their PCBs under TPPC, FTPPC, EPPC and SFPPC, respectively, implying that the proposed SFPPC method still maintains good initial transient performance while removing the limitation existing in TPPC [11], FTPPC [35] and EPPC [38] methods. Furthermore, the "flexibility" of the presented SFPPC approach is also verified by comparing it with the method in [39]. One can see from Fig.10 that when the input is saturated, the singularity will appear under the PPC method proposed in [39], resulting in the termination of simulation, while the proposed SFPPC method is still valid.

V. Conclusion

This article first proposes a SFPPC algorithm of ISNSs. By designing a new pair of SFPCBs, which can not only adaptively slide the initial PCBs according to the initial error state to satisfy any bounded initial error constraint without sacrificing the transient performance, but also adaptively adjust the PCBs according to the input saturation condition to

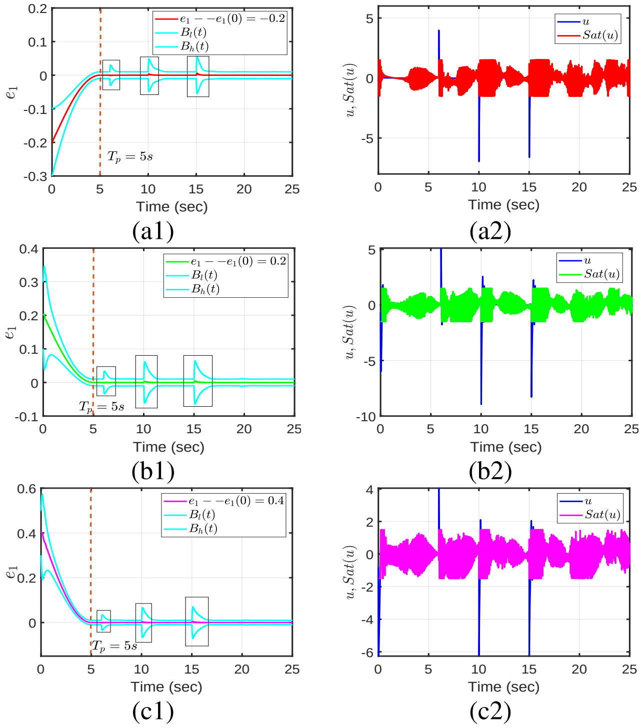

Fig. 8: (aj)(bj)(cj) with $j = 1, 2$ represent tracking error curves and control input curves under the three initial error conditions $e_1(0) = -0.2, e_1(0) = 0.2$, and $e_1(0) = 0.4$, respectively.

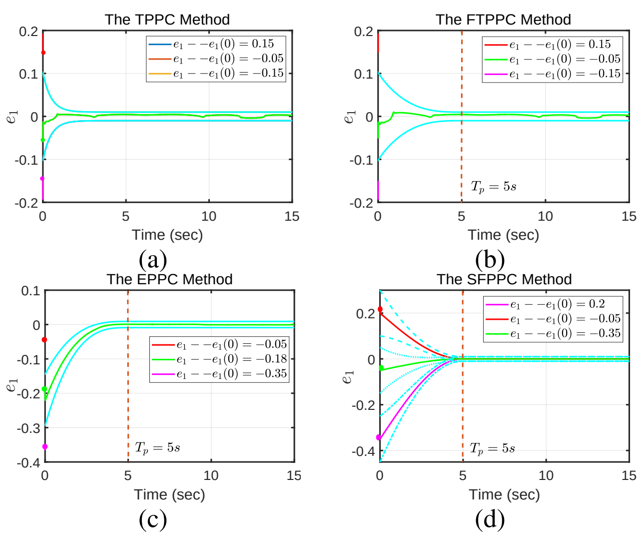

Fig. 9: (a)-(d) represent the tracking error curves and their PCBs under TPPC, FTPPC, EPPC and SFPPC with different initial conditions respectively.

achieve the balance between the performance constraint and input saturation. The results show that the presented SFPPC approach can be applied to ISNSs with arbitrary initial errors without sacrificing the initial control performance, and also achieves a trade-off between performance constraint and input saturation. The sliding flexible prescribed performance output feedback control and application of ISNSs will be the direction of our future efforts.

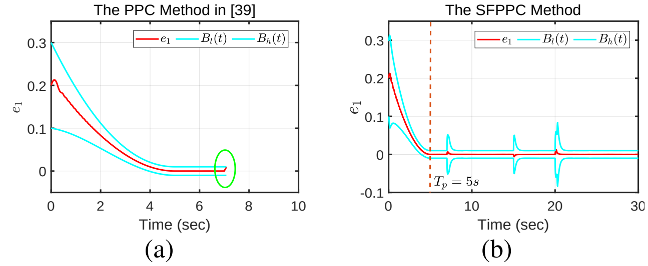

Fig. 10: (a)(b) respectively represent the tracking error curves of the PPC method in [39] and the proposed SFPPC method.

REFERENCES

[1] K.B. Ngo, R. Mahony and Z.P. Jiang, "Integrator backstepping using barrier functions for systems with multiple state constraints," in *Proceedings of the 44th IEEE Conference on Decision and Control*, Seville, Spain, 2005, pp.8306-8312.

[2] Y. Liu, Y. Wang, Y. Feng and Y. Wu, "Neural network-based adaptive boundary control of a flexible riser with input deadzone and output constraint," *IEEE Trans. Cybern.*, vol.52, no.12, pp.13120-13128, Dec.2022.

[3] S. Ding, B. Zhang, K. Mei and J.H. Park, "Adaptive fuzzy SOSM controller design with output constraints," IEEE Trans. Fuzzy Syst., vol. 30, no. 7, pp. 2300-2311, July 2022.

[4] Y. Mei, Y. Liu, H. Wang and H. Cai, "Adaptive deformation control of a flexible variable-length rotary crane arm with asymmetric input-output constraints," *IEEE Trans Cybern.*, vol.52, no.12, pp.13752-13761, Dec.2022.

[5] K. Zhao and Y. Song, "Removing the feasibility conditions imposed on tracking control designs for state-constrained strict-feedback systems", *IEEE Trans. Autom. Control*, vol.64, no.3, pp.1265-1272, Mar.2019.

[6] K. Zhao, L. Chen and C. L. P. Chen, "Event-based adaptive neural control of nonlinear systems with deferred constraint," *IEEE Trans. Syst.,Man, Cybern.: Syst.*, vol.52, no.10, pp.6273-6282, Oct.2022.

[7] Y.G. Yao, J.Q. Tan, J. Wu and X. Zhang, " A unified fuzzy control approach for stochastic high-order nonlinear systems with or without state wonstraints," *TEEE Trans Fuzzy Syst.*, vol.30, no.10, pp.4530-4540, Oct.2022.

[8] Y.G. Yao, Y. Kang, Y.B. Zhao, P.F. Li and J.Q. Tan,"Unified fuzzy control of high-order nonlinear systems with multi-type state constraints," *IEEE Trans. Cybern.*, vol.54, no.4, pp.2525-2535, Apr.2024.

[9] Y.G.Yao, J.Q. Tan, J.Wu and X.Zhang, "Decentralized fixed-time control for state-constrained stochastic systems via nonlinear state-dependent function approach," *Int. J. Robust Nonlinear Control*, vol.32, no.8, pp.4923-4945, May.2022.

[10] Y.G.Yao, J.Q. Tan, J.Wu and X.Zhang, "Event-triggered fixed-time adaptive fuzzy control for state-constrained stochastic nonlinear systems without feasibility conditions," *Nonlinear Dyn.*, vol.105, pp.403-416, Jun.2021.

[11] C.P. Bechlioulis, G.A. Rovithakis, "Robust adaptive control of feedback linearizable MIMO nonlinear systems with prescribed performance," *IEEE Trans. Autom. Control*, vol.53, no.9, pp.2090-2099, Oct.2008.

[12] Y.L. Liu, H.J. Ma, "Adaptive fuzzy tracking control of nonlinear switched stochastic systems with prescribed performance and unknown control directions," *IEEE Trans. Syst. Man Cybern. Syst.*, vol.50, no.2, pp.590-599, Feb.2020.

[13] C. Hua, L. Zhang and X. Guan, "Decentralized output feedback adaptive NN tracking control for time-delay stochastic nonlinear systems with prescribed performance," *IEEE Trans. Neural Netw. Learning Syst.*, vol.26, no.11, pp.2749-2759, Nov.2015.

[14] W.J. Si, D.X. Dong and F.F.Yang, "Decentralized adaptive neural prescribed performance control for high-order stochastic switched nonlinear interconnected systems with unknown system dynamics," *ISA Trans.*, vol.84, pp.55-68, Jan.2019.

[15] Q. Zhou, H. Li, L. Wang and R. Lu, "Prescribed performance observer-based adaptive fuzzy control for nonstrict-feedback stochastic nonlinear systems," *IEEE Trans. Syst., Man, Cybern, Syst.*, vol.48, no.10, pp.1747-1758, Oct.2018.

[16] A. Polyakov, D. Efimov and W. Perruquetti, "Finite-time and fixed-time stabilization: implicit Lyapunov function approach," *Automatica*, vol.51, pp.332-340, Jan.2015.

[17] M. Cai, P. Shi and J. Yu, "Adaptive neural finite-time control of non-strict feedback nonlinear systems with non-symmetrical dead-zone," *IEEE Trans. Neural Netw. Learning Syst*., vol.35, no.1, pp.1409-1414, Jun.2024.

[18] Y.G.Yao, J.Q. Tan, J.Wu, X.Zhang and L.He, "Prescribed tracking error fixed-time control of stochastic nonlinear systems," *Chaos Solitons Fractals*, vol.160, 112288, Jul.2022.

[19] Y.G.Yao, J.Q. Tan, J.Wu and X.Zhang, "Event-triggered fixed-time adaptive neural dynamic surface control for stochastic non-triangular structure nonlinear systems," *Inf.Sci*., vol.569, pp.527-543, Aug.2021.

[20] Z. Cuan, D.W. Ding, Y. Ren and X.J. Li, "Adaptive fixed-time control for state-constrained high-order uncertain nonlinear cyber-physical systems under malicious attacks," *IEEE Trans. Fuzzy Syst*., 2023, doi: 10.1109/TFUZZ.2023.3281605.

[21] J.D. Snchez-Torres, E.N. Sanchez, and A.G. Loukianov, "Predefined-time stability of dynamical systems with sliding modes," in *2015 American control conference (ACC)*, pp.5842-5846, IEEE, 2015.

[22] Y.D. Song, Y.J. Wang, J. Holloway and M. Krstic, "Time-varying feedback for regulation of normal-form nonlinear systems in prescribed finite time," *Automatica*, vol.83, pp.243-252, Sep.2017.

[23] C.C. Hua, P.J. Ning and K. Li, "Adaptive prescribed-time control for a class of uncertain nonlinear systems," *IEEE Trans. Autom. Control*, vol.61, no.17, pp.6159-6166, Nov.2021.

[24] W. Li and M. Krstic, "Prescribed-time output-feedback control of stochastic nonlinear systems," *IEEE Trans. Autom. Control*, vol.68, no.3, pp.1431-1446, Mar.2023.

[25] Y.G. Yao, Y. Kang, Y.B. Zhao, P.F. Li and J.Q. Tan, "Prescribed-time output feedback control for cyber-physical systems under output constraints and malicious attacks," IEEE Trans.Cybern., 2024, doi:10.1109/TCYB.2024.3418384.

[26] Y.G. Yao, Y. Kang, Y.B. Zhao, P.F. Li and J.Q. Tan, "A novel prescribed-time control approach of state-constrained high-order nonlinear systems," *IEEE Trans. Syst., Man, Cybern.: Syst.,* 2024, doi: 10.1109/TSMC.2024.3352905.

[27] S. Sui, C.L.P. Chen and S. Tong, "Finite-time adaptive fuzzy prescribed performance control for high-order stochastic nonlinear systems," *IEEE Trans. Fuzzy Syst*., vol.30, no.7, pp.2227-2240, Jul.2022.

[28] B. Xin, S. Cheng, Q. Wang, J. Chen and F. Deng, "Fixed-time prescribed performance consensus control for multiagent systems with nonaffine faults," *IEEE Trans. Fuzzy Syst*., vol.31, no.10, pp.3433-3446, Oct.2023.

[29] Z. Liang, Z. Wang, J. Zhao, P.K. Wong, Z. Yang and Z. Ding, "Fixed-time and fault-tolerant path-following control for autonomous vehicles with unknown parameters subject to prescribed performance," *IEEE Trans. Syst., Man, Cybern Syst*., vol.53, no.4, pp.2363-2373, Apr.2023.

[30] H. Duan, Y. Yuan and Z. Zeng, "Distributed robust learning control for multiple unmanned surface vessels with fixed-time prescribed performance," *IEEE Trans. Syst., Man, Cybern.: Syst*., 2023,doi: 10.1109/TSMC.2023.3321119.

[31] Y. Liu, X.P. Liu and Y.W. Jing, "Adaptive neural networks finite-time tracking control for non-strict feedback systems via prescribed performance," *Inf. Sci*., vol.468, pp.29-46, Nov.2018.

[32] Y. Liu, X. Liu, Y. Jing, X. Chen and J. Qiu, "Direct adaptive preassigned finite-time control with time-delay and quantized input using neural network," *IEEE Trans. Neural Netw. Learning Syst*., vol.31, no.4, pp.1222-1231, Apr.2020.

[33] K. Sun, R. Guo and J. Qiu, "Fuzzy adaptive switching control for stochastic systems with finite-time prescribed performance," *IEEE Trans. Cybern*., vol.52, no.9, pp.9922-9930, Sep.2022.

[34] Y.G.Yao, J.Q. Tan, J.Wu and X.Zhang, "Event-triggered finite-time adaptive fuzzy tracking control for stochastic nontriangular structure nonlinear systems," *Int. J. Fuzzy syst*., vol.23, pp.2157-2169, Jun.2021.

[35] J.X. Zhang and T. Chai, "Proportional-integral funnel control of unknown lower-triangular nonlinear systems," *IEEE Trans. Autom.Control*, vol. 69, no. 3, pp. 1921C1927, Mar. 2024.

[36] S. Sui, C. L.P. Chen and S. Tong, "A novel full errors fixed-time control for constraint nonlinear systems," *IEEE Trans. Autom. Control*, vol.68, no.4, pp.2568-2575, Apr.2023.

[37] K. Zhao, F. Lewis and L. Zhao, "Unifying performance specifications in tracking control of MIMO nonlinear systems with actuation faults,"*Automatica*, vol.155, 111102, Sep. 2023.

[38] Y. Shi, B.W. Yi, W. Xie and W.D. Zhang, "Enhancing prescribed performance of tracking control using monotone tube boundaries," *Automatica*, vol.159, 111304, Jan.2024.

[39] H. Xie, Y. Jing, J. X. Zhang and G. M. Dimirovski, "Low-complexity tracking control of unknown strict-feedback systems with quantitative performance guarantees," *IEEE Trans. Cybern*., doi: 10.1109/TCYB.2024.3390440.

[40] W. Zhang and W. Wei, "Disturbance-observer-based finite-time adaptive fuzzy control for non-triangular switched nonlinear systems with input saturation," *Inf. Sci*., vol.561, pp.152-167, Jun.2021.

[41] G. Zong, Q. Xu, X. Zhao, S.F. Su, and L. Song, "Output-feedback adaptive neural network control for uncertain nonsmooth nonlinear systems with input deadzone and saturation," *IEEE Trans. Cybern*., vol.53, no.9, pp.5957-5969, Sep.2023.

[42] Y.F. Gao, X.M. Sun, C. Wen, and W. Wang, "Adaptive tracking control for a class of stochastic uncertain nonlinear systems with input saturation," *IEEE Trans. Autom. Control*, vol.62, no.5, pp.2498-2504, May.2017.

[43] Y. Yang, J. Tan, and D. Yue, "Prescribed performance tracking control of a class of uncertain pure-feedback nonlinear systems with input saturation," *IEEE Trans. Syst., Man, Cybern. Syst*., vol.50, no.5, pp.1733-1745, May.2020.

[44] Y. Sun, J. Liu, Y. Gao, Z. Liu and Y. Zhao, "Adaptive neural tracking control for manipulators with prescribed performance under input saturation," *IEEE/ASME Trans. Mechatronics*, vol.28, no.2, pp.1037-1046, Apr.2023.

[45] H. Shen, X. Yu, H. Yan, J. H. Park and J. Wang, "Robust fixed-time sliding mode attitude control for a 2-DOF helicopter subject to input saturation and prescribed performance," *IEEE Trans. Transport. Electrific*., 2024, doi: 10.1109/TTE.2024.3402316.

[46] K. Yong, M. Chen, Y. Shi, and Q. Wu, "Flexible performance-based robust control for a class of nonlinear systems with input saturation," *Automatica*, vol.122, 109268, Dec.2020.

[47] Y.G. Yao, Y. Kang, Y.B. Zhao, P.F. Li and J.Q. Tan, "Flexible prescribed performance output feedback control for nonlinear systems with input saturation," *IEEE Trans. Fuzzy Syst*., 2024, doi: 10.1109/TFUZZ.2024.3418772.

[48] X. Yue, H. Zhang, J. Sun and L. Wan, "Adaptive event-triggered saturation-tolerant control for multi-agent systems based on finite-time fuzzy learning," *IEEE Trans. Fuzzy Syst*., doi: 10.1109/TFUZZ.2024.3423347.

[49] R. Ji, D. Li and S.S. Ge, "Saturation-tolerant prescribed control for nonlinear time-delay systems," *IEEE Trans. Fuzzy Syst*., vol.31, no.8, pp.2495-2508, Aug.2023.

[50] H. Xie, G. Zong, D. Yang, X. Zhao and Y. Yi, "Flexible-fixed-time-performance-based adaptive asymptotic tracking control of switched nonlinear systems with input saturation," *IEEE Trans. Autom. Sci. Eng*., 2023, doi: 10.1109/TASE.2023.3324953.